

# Cathode Erosion Studies on MPD Thrusters

H. O. Schrade,\* M. Auweter-Kurtz,† and H. L. Kurtz†  
*University of Stuttgart, Federal Republic of Germany*

**The fundamental processes occurring at the cathode interphase of magnetoplasmadynamic (MPD) arcs and their consequences on material erosion are by no means fully understood, despite the great many publications in this field on various different arc types of similar conditions. This paper presents the results of a cathode erosion study on an MPD arc thruster under pulsed and steady-state operating modes and, moreover, gives an explanation of the cathode attachment mechanisms for both operating modes.**

## Introduction

It is a known phenomenon that in a pulsed MPD thruster<sup>1-3</sup> and during the starting phase in a continuous MPD thruster,<sup>4,5</sup> the arc cathode attachment resembles many hot spots of high current density. These spots are usually highly nonstationary and jump across the cathode surface. Such a spotty attachment is indeed the most common one on cold metal cathodes of low-pressure arcs,<sup>6,7</sup> and seems to be an intrinsic feature of those discharges. Despite the growing literature on this phenomenon, it is still not fully understood. However, since the time resolution of electrical and optical measuring techniques went up into the microsecond and even beyond the nanosecond range, and since scanning electron microscopy became a widespread technique of investigating the arc traces left on cathode surfaces, one has learned much more on the mechanisms of this spotty attachment. Today one distinguishes between 1) microspots with diameters of several micrometers (maybe even less) and with current densities of the order of  $10^{12}$  A/m<sup>2</sup> (maybe even higher) and displacement velocities of several hundred meters per second, and 2) spots that are much more stationary (velocities of the order of several meters per second) with diameters of up to 100  $\mu$ m.<sup>8</sup> These latter, larger spots appear to be the result of spot clustering; i.e., due to favorable emission conditions, the microspots do not spread over a larger area but rather stick to a smaller area, and by locally overheating this area cause larger molten zones and relatively heavy damage to the cathode. If such a clustering does not occur, the microspot damage is less severe because of the rapid spot motion and because, consequently, there is more widespread averaged heat load on the cathode surface.

Another quite interesting feature is the fact that the average number of spots is proportional to the arc current, and that a single spot can carry only a limited current, the quantity of which depends on the cathode material.<sup>9,10</sup>

Within a transverse magnetic field, these spots jump preferably into the retrograde direction, i.e., they move oppositely to Ampere's law, as long as the ambient pressure is small enough.<sup>11,12</sup>

These are only some of the most striking known and established effects observed on spotty cathodes. Many more detailed spot features have been observed and put forward,

but they cannot be dealt with in the framework of this paper. Therefore, reference shall be made to the literature.<sup>7</sup>

Nevertheless, since a variety of these effects are obviously involved at the cathode-arc interphase of magnetoplasmadynamic (MPD) thrusters, it is mandatory that this spot behavior be investigated in order to understand and predict the discharge and erosion effects during the starting phase of a continuously running MPD arc thruster or during the pulse phase of a quasisteady MPD arc thruster.

After the starting phase of a continuously running thruster, which lasts about a fraction of a second or a few seconds depending on the arc current, the cathode, which usually consists of a thoriated tungsten rod—so far the only successfully used in continuous thrusters—starts to glow, and the original spotty attachment becomes a quiet, more diffuse one. The current densities of these diffuse attachments on bright glowing tungsten cathodes are of the order of  $10^7$  A/m<sup>2</sup> and are commonly explained by thermionic emission,<sup>4</sup> while the high current densities of the spots can be interpreted only by means of field or enhanced thermal field emission.<sup>13,14</sup>

The following section reports about erosion measurements on pulsed and continuous MPD thrusters and consequently on spotty and diffuse cathode attachments, while the subsequent sections give a partially quantitative theoretical interpretation and discussion of the experimental findings.

## Experiment

The cathode erosion tests have been conducted on a nozzle-type MPD thruster,<sup>15</sup> as shown in Fig. 1. The center cathode consists of a thoriated tungsten rod (98% W,  $\approx 2\%$  ThO<sub>2</sub>) which is casted into a copper support. The copper support with the tungsten rod are finally screwed onto a water-cooled copper rod and can be loosened for weighing. The propellant, argon, is fed along the cathode rod into the arc chamber. The arc chamber and nozzle are built of individually water-cooled and insulated copper segments. The last segment of the nozzle exit represents the anode. For the pulsed thruster experiments, the water-cooled segments up to the anode ring have been replaced by a heat-resistant glass ceramic (MACOR) and the water cooling in anode and cathode not applied. The eroded mass is determined by weighing the cathode before and after the experiment with a precision balance having an accuracy of 1 mg at a weighing range of 1 kg.

### Steady-State MPD Thruster

With steady-state operating MPD thrusters, two different modes of erosion must be distinguished:

1) Starting with a cold cathode, heavy erosion takes place, which can usually be detected as a sort of "spitting" of glowing particles or droplets. Some tenth of a second to

Presented as Paper 85-2019 at the AIAA/DGLR/JSASS 18th International Electric Propulsion Conference, Alexandria, VA, Sept. 30–Oct. 2, 1985; received Dec. 4 1985; revision submitted Oct. 15, 1986. Copyright © American Institute of Aeronautics and Astronautics, Inc., 1986. All rights reserved.

\*Senior Scientist, Vice Director, Institute for Space Systems. Member AIAA.

†Staff Scientist, Institute for Space Systems.

several seconds later, the cathode tip becomes hot and glowing so that thermionic or enhanced thermal field emission can occur, and the discharge becomes stable and quiet.

2) During the steady-state operation phase, the arc attachment is confined to the bright glowing area of the cathode tip. The erosion effect is much smaller, and no glowing particles are ejected. To measure these different erosion rates, two series of tests were performed: long duration and start-only runs.

#### Erosion During Starting Phase

During the "start-up phase," the arc attachment consists of many highly unstationary hot spots, which jump over the cathode surface and cause a relatively high evaporation and even splashing of cathode material.

A current voltage plot of this initial starting phase ( $0 \leq t \leq t_f$ ) is shown in Fig. 2. To determine the average erosion rate during this starting phase, experiments with 30–50 runs with different preset ignition currents were performed. In each case, the arc was extinguished after stabilization. To exclude eventual thermal effects in the starting phase, a waiting period of about 10 min was taken between the tests to cool down the cathode. Depending now on the ignition current  $I_f$  set by the power supply, the time duration  $t_f$  of the starting phase, i.e., the time to heat up the cathode, varies between about a fraction of a second and several seconds; a simple curve fit of these measurements is shown in Fig. 3.

Based on these experiments, it became clear that, by far, the major erosion takes place during the starting phase when the cathode is still fairly cold and a spotty discharge exists.

In Figs. 4 and 5, the average mass loss is plotted after about 30–50 runs as a function of the ignition current and the corresponding accumulated charge during the starting phases, respectively. The total average mass loss per arc ignition amounts to about 25 mg for a preset arc ignition current of 600 A and decreases to about 10 mg, and to a little less if the ignition current is 1000 A and more. Since with increasing current  $I_f$  the cathode heats up faster, and therefore the time elapsed during the starting phase becomes smaller, the total mass loss decreases with increasing ignition current. As a function of the accumulated electric charge  $\bar{Q}_f$ , however, the mass loss increases with  $\bar{Q}_f$  almost linearly. By taking the least-square fit slope, we obtain an average erosion rate for the starting or initial phase of  $16.7 \mu\text{g/C}$ .

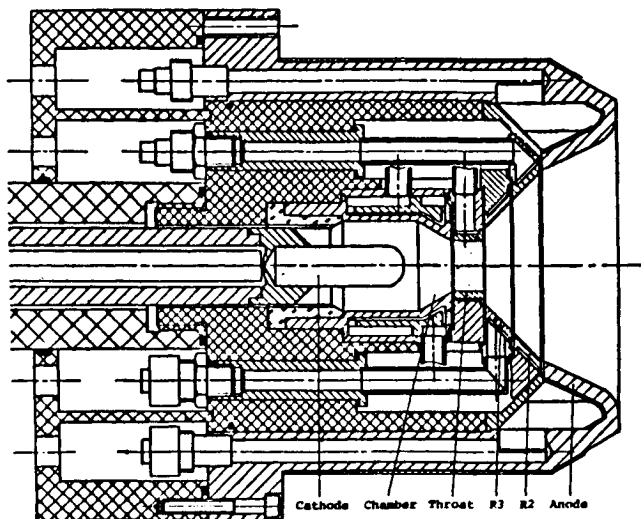


Fig. 1 Self-field MPD thruster head schematic.

#### Erosion During Steady-State Operation

During the long duration tests, lasting about 240–60 minutes at steady-state currents between 1500 and about 4000 A, respectively, i.e., below onset conditions (since steady-state MPD thrusters must be run below onset to avoid destruction), the measured total mass loss is about 400 mg. The erosion rate—not counting the losses of the starting phase—amounts to about  $0.03 \mu\text{g/C}$ , which is three orders of magnitude below that of the ignition phase. The measured erosion rates, given by the cathode mass loss  $\Delta m$  divided by the accumulated electric charge  $Q$  in  $\mu\text{g/C}$ , for the continuously running steady-state arc are plotted as a function of arc power in Fig. 6. The erosion rate may be considered a constant, and as shown in the case of the arc power  $P$ , it is also independent of the arc current  $I$  and the correlation

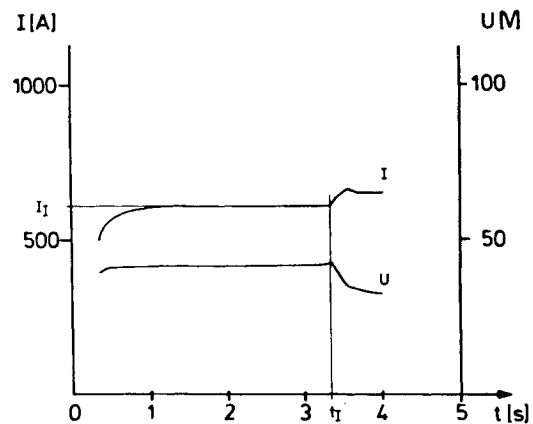


Fig. 2 Typical current and voltage traces during starting phase.

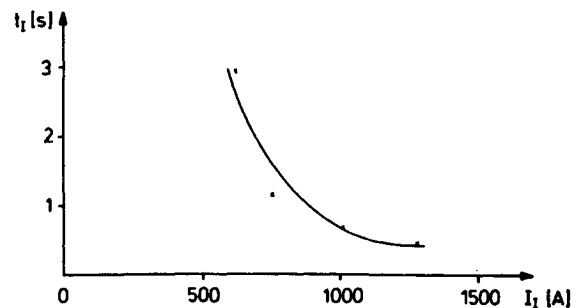


Fig. 3 Starting phase duration as a function of ignition current  $I_f$ .

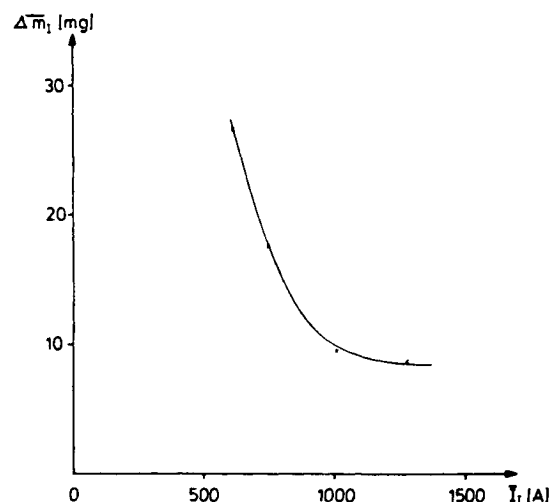


Fig. 4 Average mass loss during starting phase as a function of the ignition current  $I_f$ .

parameter  $I^2/\dot{m}$ , i.e., one may conclude that the mass loss per unit time,  $\dot{m}_v = \Delta m / \Delta t$ , is proportional to the current. Since  $Q = I \Delta t$ , one obtains a mass loss rate of about

$$\dot{m}_v = \Delta m / \Delta t = 0.03 \cdot I \quad [\mu\text{g/s}] \quad (1)$$

for the continuously running steady-state thruster.

#### Quasisteady MPD Thruster

Measurements on a pulsed thruster with the same electrode material and geometry<sup>16</sup> show an average erosion rate of about  $14 (\pm 3.5) \mu\text{g/C}$  with argon as the propellant and  $16 (\pm 3.5) \mu\text{g/C}$  with nitrogen as the propellant (see Fig. 7). These latter results were obtained by weighing the cathode before and after about 420 shots at the same operation conditions. The pulsed thruster was energized by a pulse-forming network with electrolytic capacitors,<sup>17</sup> which produces rectangular current pulses of up to  $I_{\text{max}} \approx 8000 \text{ A}$  lasting about 2 ms. It is interesting to note that the erosion rate measured for the pulsed thruster is about the same as that for the initial phase of the continuous thruster, but also is a factor of 3–5 greater than the erosion measured in Japan with quasisteady thrusters.<sup>1,2</sup>

In the following section, an explanation of 1) the spotty "cold-cathode attachment" with a fairly high erosion rate and 2) the more diffuse "hot-cathode attachment" of much lower erosion will be presented.

#### Theory

Based on the experimental findings, one distinguishes between 1) a spotty, more or less highly erosive, and 2) a

bright glowing diffuse, low erosive cathode attachment within a MPD arc thruster. First, let us consider the spotty arc cathode.

#### Cold Spotty Arc Cathode

The starting phase of an MPD arc may be described by the following: at any favored spot (microprotrusion and/or dielectric impurity) on the cathode surface, the electric field becomes strong enough to start a breakdown. This breakdown causes a local overheating of the emitting, microscopic spot site, thus leading to evaporation and a plasma cloud, which expands from the spot site on the cathode surface into the gaseous half-space. After this first ignition phase, which according to Guile and Jüttner<sup>6</sup> may last about  $10^{-9} \text{ s}$ , a small crater with a diameter of a few microns is formed (see Fig. 8). A few typical, but more developed, craters left on the surface of a thoriated tungsten cathode are shown in the photomicrograph of Fig. 9.

The high-pressure quasineutral vapor plasma is now interconnected with the overheated and molten inner crater surface by a space-charge layer with a thickness of several Debye length. The electric field  $E_0$ , which is caused by the space-charge layer on the surface of a planar cathode, can now be calculated as a function of the electron and ion temperatures  $T_e$  and  $T_i$  (Kelvin), the ion mass  $m_i$ , and the Debye length  $\lambda_D$ ; it is<sup>18</sup>

$$E_0 = \frac{kT_e}{e} \frac{1}{\lambda_D} \left[ \sqrt{\frac{m_i T_e}{m_e T_i}} - 1 \right]^{1/2} \\ = 2.03 \times 10^7 \left[ \sqrt{M_i \frac{T_e}{T_i}} - 0.0234 \right]^{1/2} \sqrt{p_e} \quad [\text{V/m}] \quad (2)$$

where  $p_e$  is the partial pressure of the electron gas, and  $M_i$  is the atomic weight of the ionized metal atoms within the

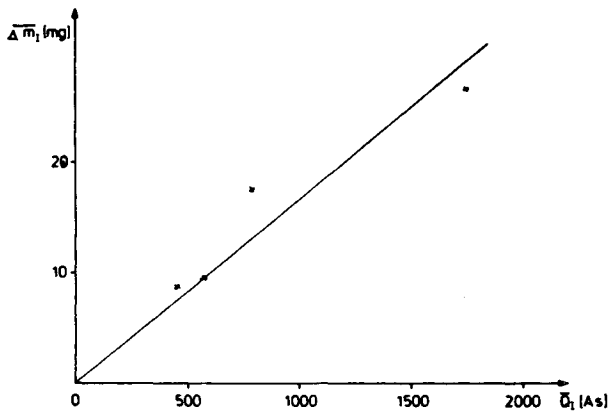


Fig. 5 Average mass loss during starting phase as a function of the accumulated charge  $Q_i$ .

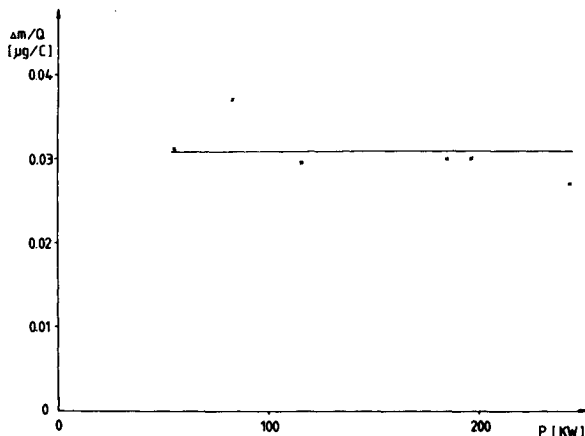


Fig. 6 Steady-state erosion rates vs arc power.

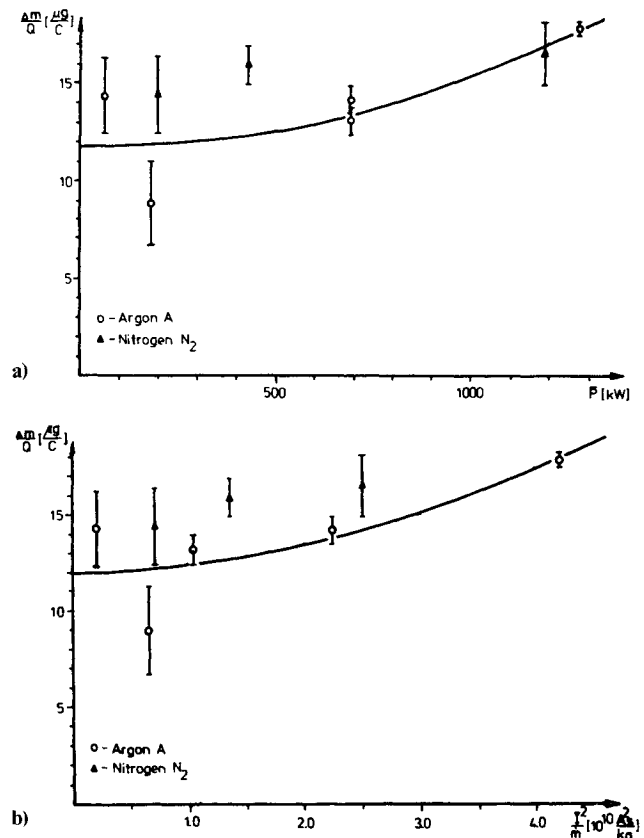


Fig. 7 Erosion rates for quasisteady operation vs a) arc power, and b) correlation parameter  $I^2/\dot{m}$ .

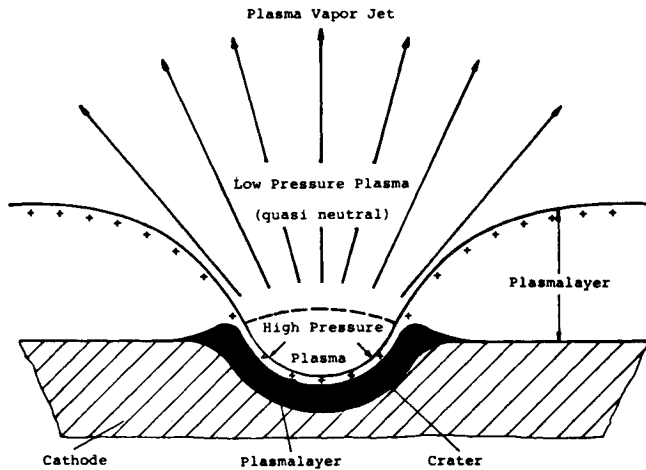


Fig. 8 Configuration of the plasma layer within and around a crater of a cathode spot.

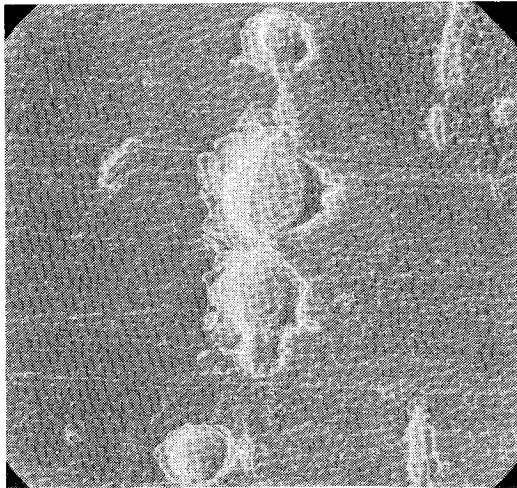


Fig. 9 Photomicrograph of a thoriated tungsten cathode surface after a pulsed arc discharge (magnification 1000).

quasineutral plasma above the surface. This relation is also valid as long as the plasma layer thickness within the crater is small compared to the crater size, or as long as the Debye length given by

$$\lambda_D = \sqrt{\frac{\epsilon_0 k T_e}{2e^2 n_e}} = \frac{k T_e}{e} \sqrt{\frac{\epsilon_0}{e p_e}} = 1.813 \times 10^{-10} \frac{T_e}{\sqrt{p_e}} \quad [\text{m}] \quad (3)$$

is much smaller than the crater radius  $r_0$ . Only in that case is the assumption of a planar cathode surface valid. Indeed, within the crater, the plasma pressure and, hence, the partial pressure of the electron gas can be considered to be much higher than outside<sup>19</sup>; therefore,  $\lambda_D$  and the thickness of the plasma layer above the inner crater surface is thin ( $\ll r_0$ ) while outside off the crater the plasma layer is relatively thick. As a consequence of this plasma boundary configuration, the electric field strength  $E_0$  on the concave crater surface is much larger than outside and therefore strong enough to maintain a high current density, due to field emission or thermal field emission on the inner crater surface. The following quantitative discussion shall corroborate this explanation.

In Fig. 10, the current density for thermal field emission is plotted as a function of the electric field strength  $E_0$  for a tungsten cathode with an electron work function of  $\phi = 4.5$  eV. In order to obtain current densities of the order of  $10^{10}$ – $10^{12}$  A/m<sup>2</sup> as found experimentally,  $E_0$  should be about

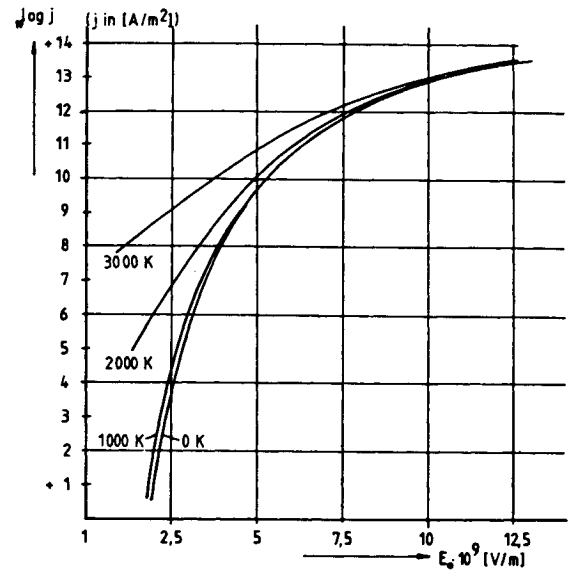


Fig. 10 Current density due to thermal field emission for an electrode work function  $\phi = 4.5$  eV (tungsten).

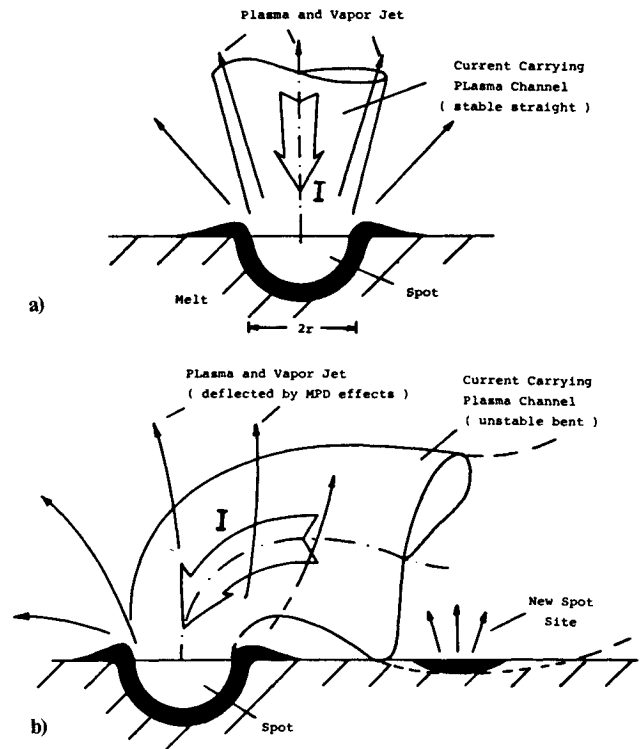


Fig. 11 a) Straight stable and b) bent unstable current-carrying plasma channel which emanates from a cathode spot.

$5\text{--}8 \times 10^9$  V/m. According to Eq. (2), a space-charge field of this strength requires a partial pressure of the electron gas of  $p_e = 4.6 \times 10^3$  to  $1.2 \times 10^4$  N/m<sup>2</sup> within the high-pressure tungsten vapor plasma. Since the plasma temperature must be taken larger than 10,000 K, this electron pressure corresponds to a plasma pressure of about 0.1–1 bar. Now the pressure of the spot plasma exceeds by far 1 bar, so that the electric field is strong enough to explain the high current densities of  $10^{12}$  A/m<sup>2</sup> (and may be even higher on certain localized areas within an active crater); moreover, it shows that the Debye length is smaller than  $\lambda_D < 0.1 \mu\text{m}$ , i.e., much smaller than the crater radius of about  $1 \mu\text{m}$ .

The concept of an active arc spot may therefore be described by a high-pressure plasma and vapor region, from which a strong jet expands out into the gaseous half-space of lower pressure. This plasma jet is current-carrying, i.e., it contains a current channel, which electrically connects the high-pressure spot plasma with the interelectrode plasma and the anode (see Fig. 11a).

The current density within this channel is, as we have seen, quite high, so that electromagnetic forces cannot be neglected. As it has been shown elsewhere<sup>19,20</sup> that such a current-carrying plasma channel with an axial flow is only straight and stable if the pressure difference between the plasma and vapor pressure  $p_v$  at the inner crater surface and the ambient pressure  $p_\infty$  is larger than (about) three times the average magnetic pressure. A more detailed investigation shows that this factor is about 3.0 for an almost flat crater (Fig. 12); for a hemispherical crater (Fig. 11a) it is about 3.3. The mathematical criterion for a stable straight discharge channel emanating from an active cathode spot follows therefore by

$$p_v - p_\infty > k(\mu_0/8\pi)I_s j_s \quad (4)$$

where  $3 \leq k \leq 3.3$ ,  $\mu_0 = 4\pi \times 10^{-7}$  Vs/Am (the magnetic permeability),  $I_s$  is the spot current, and  $j_s$  is the average current density across the spot orifice. Since for any arc spot the ambient pressure  $p_\infty$  can be assumed small compared to the spot pressure  $p_v$  above the melt, the value of the product spot current times current density, at which a spot discharge goes from stable to unstable, can be directly related to  $p_v$ .

In Fig. 13, the vapor pressure curves or the spot conditions  $p_v$  and  $T_s$  for stable and unstable behavior on pure metal cathodes, such as copper molybdenum and tungsten, are illustrated. Below these curves, a spot discharge is stable; above these curves it is unstable and cannot exist.

If the preceding criterion [Eq. (4)] is not fulfilled, any small disturbance leading to a minute curvature causes the current-carrying plasma channel to kink, i.e., the channel axis bends more and more and eventually the channel will come in contact with the cathode surface at a nearby site off the original spot (Fig. 11b). The new site will be heated up and a new current-carrying spot will be initiated. Again, for this new spot, the stability requirement [Eq. (4)] must be fulfilled in order to maintain a stable and active discharge.

Thus, by increasing the arc current  $I$  higher and higher, one has to expect that more and more microspots are created, which now spread over the cathode surface and/or cluster together as larger spots. The clustered or larger spots can now have features similar to the microspots. Again, a plasma and vapor jet will propagate from a clustered spot (Fig. 12) and, for the main current-carrying channel, which emanates from this larger spot site, the same stability criteria [Eq. (4)] as derived for the microspot is now applicable. Therefore, one may state that the requirement [Eq. (4)] is valid very generally for any stable type of cathode spot. For the clustered or larger spots, however, their total spot current,  $I_s$ , will be larger, while the average current density,  $j_s$ , becomes smaller than in the case of a microspot.

The vapor pressure above the melt  $p_v$  in Eq. (4) can now be related to the evaporation rate and to the average surface temperature  $T_s$  of the spot. Hence, the stability criteria (4) can also be written in the form

$$\dot{m}_{vs} \geq \frac{\mu_0}{8\pi} \sqrt{\frac{M}{2\pi R T_s}} I_s^2 g k \left\{ 1 + \frac{p_\infty}{k(\mu_0/8\pi)I_s j_s} \right\} \quad (5)$$

where  $\dot{m}_{vs}$  is the cathode material, evaporated per second, of the spot,  $M$  is the molecular or atomic weight of the vapor,  $R$  is the universal gas constant and  $g$ , like  $k$ , is a geometric factor, which now varies between 1 and 2 depending on the presence of a flat (Fig. 12) or hemispherical (Fig. 11a) spot

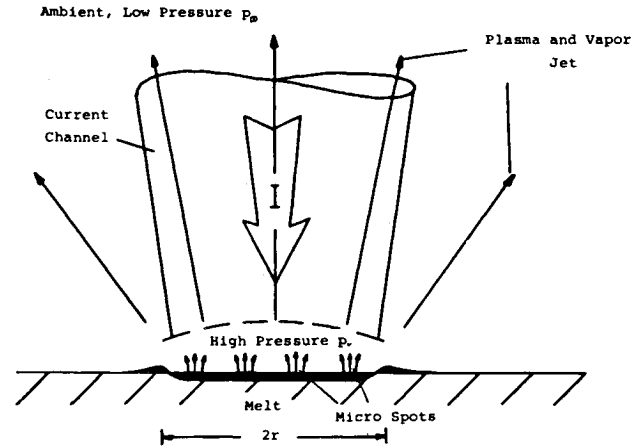


Fig. 12 Clustered spot.

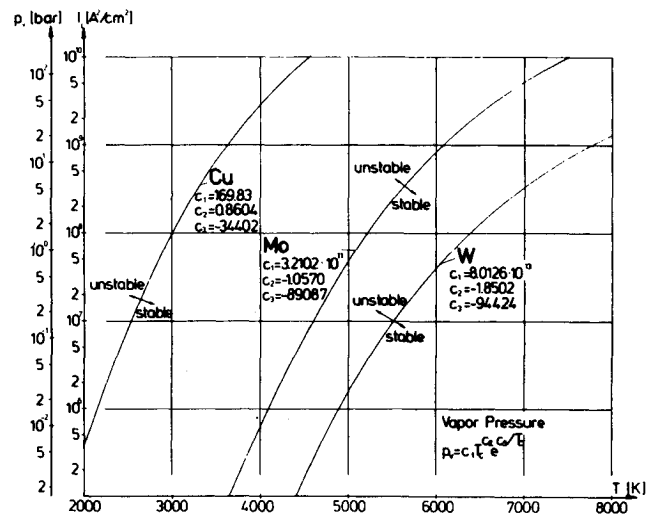


Fig. 13 Vapor pressure and critical quantity  $Ij$  which can be carried by one spot for different electrode materials.

profile. Since the magnetic pressure at the spot is larger than the ambient pressure (this requirement follows practically by definition of a spot discharge and is experimentally verified), one can neglect the second term in the brace expression of Eq. (5) and can obtain the stability requirement for a spot by

$$\dot{m}_{vs} > \dot{m}_{vs,min} = c\sqrt{M/T_s} I_s^2 \quad [\text{kg/s}] \quad (6)$$

Herein the constant  $c$  is about  $0.66 \times 10^{-9}$  [kg K<sup>1/2</sup>/(A<sup>2</sup>s)] for a flat spot and  $1.4 \times 10^{-9}$  [kg K<sup>1/2</sup>/(A<sup>2</sup>s)] for a hemispherical one. A spot discharge therefore always requires a minimum evaporation rate  $\dot{m}_{vs,min}$ , which is proportional to the square root of the molecular or atomic weight  $M$  of the evaporated cathode material and inversely proportional to the square root of the melted spot surface temperature,  $T_s$ . If the cathode attachment consists of  $n$  individual spots identified by the indices 1,2,...,i,...,n, the overall minimum evaporation rate follows by

$$\dot{m}_{v,min} = \sum_{i=1}^n \dot{m}_{vi,min} = c \sum_{i=1}^n \sqrt{M/T_{si}} I_{si}^2 \quad (7)$$

and since the total current  $I$  is given by the sum over all spot currents  $I_s$ , the overall minimum erosion rate due to evaporation,  $\epsilon_{v,min}$ , is, by definition,

$$\epsilon_{v,min} = \frac{\dot{m}_{v,min}}{I} = c \left[ \sum_{i=1}^n \sqrt{M/T_{si}} I_{si}^2 / \sum_{i=1}^n I_{si} \right] \quad [\text{kg/C}] \quad (8)$$

It is of interest to note that, according to Eq. (8), the spots with relatively high individual current rates ( $I_{si}$  large), i.e., the clustered spots, contribute the major amount of erosion, and that the erosion rate is about proportional to the spot current to those spots. If the cathode attachment consists only of many identical microspots with the same average spot current,  $I_{si} = I_s = \text{const}$ , and the same average surface temperature  $T_{si} = T_s = \text{const}$ , the overall erosion rate becomes independent of the number of spots and reduces to

$$\epsilon_{v,\min} = c\sqrt{M/T_s} I_s \quad [\text{kg/C}] \quad (9)$$

Therefore, the smaller the spot current, the smaller the erosion rate. This does not mean that the overall arc current must be small, but rather that the number of spots is large.

In order to avoid strong erosion in the presence of spots, it is therefore necessary to avoid clustering and to strive for many similar small spots, which are homogeneously distributed over the cathode surface and which already become unstable at a small spot current.

Let us now discuss the experimental findings on the basis of these theoretical entities. At first the *starting phase*: just after ignition there exists one microspot. The spot current increases up to a level at which the stability criteria [Eqs. (4) and (6)] are still fulfilled. If the current is increased above that level, the current-carrying plasma channel, which emanates from the spot crater, becomes unstable. It bends more and more and eventually touches the cathode surface somewhere in the vicinity of the spot. Thereby, the cathode is heated up, the plasma and vapor pressure increase and since the Debye length on the touchdown area becomes very small, a new breakdown and second spot will be initiated. Each of both spots now carries a part of the electric current so that both are stable. By further increasing the current, at least one of the spots will split again. The number of spots will now rise until the final current set by the power supply is reached.

The cathode surface will therefore be covered more and more by these microspots, which now, probably due to local accumulation of molten electrode material, cluster together and build larger spots. These clustered spots have now a higher evaporation rate and, as known from observations, these spots can also eject droplets which can increase the mass loss by almost a factor of 5.<sup>21</sup> Since during the starting phase the measured erosion rate is  $16.7 \mu\text{g/C}$ , one can now estimate the average spot current by means of Eq. (9). With the atomic weight of tungsten,  $M=184$ , and a spot temperature of 7000 K, which corresponds to the boiling point at the expected spot pressures of 10 bar, the current carried by one spot amounts to less than  $\sim 160$  A. If a droplet loss factor of about 5 were taken into account, the spot current would even sink below 32 A. Hence, the number of spots during the starting phase by a current setting of 600 A lies between about 3 and 20 spots and for a current setting of 1500 A between about 9 and 47 at least.

Similar conditions must exist now on the tungsten cathodes of *pulsed thrusters*, since during the short discharge

the cathode does not heat up to thermionic temperatures. Again, spots are present, and since the measured erosion rate is of about the same amount ( $14 \mu\text{g/C}$ ) and the spot temperature  $T_s$  must be taken about the same (since the dissipation mechanisms within spots of the same erosion rate are the same), the spot current amounts again to about 135 A or to 27 A with a droplet loss factor of 5. At the current maximum of 8000 A, the number of spots are therefore between 60 and 300. Since the conditions in all these spots vary slightly, they are not stable but should rather jump according to the following explanation. If, for instance, the plasma pressure within a spot increases slightly, the Debye length and therefore the electric resistance of the spot decreases. According to Kirchhoff's distribution law, the current will be concentrated through that circuit of lowest resistance—in our case, through the spot of lowest resistance. That means, however, that for this spot the right side of the stability requirement [Eqs. (4–6)] increases faster than the left side. The consequence will be that the discharge channel above the spot will become unstable and, hence, causes a splitting or a jump to a new spot site. The spots are therefore distributed and may jump over the cathode surface, but according to inhomogeneities of the cathode surface and of the surface cooling, as well as the entire arc shape, they will prefer to appear on certain favorable, still hard to predict areas.

Today the interdependence of all these effects and also that among spots are still not well understood. Therefore, a sound prediction of spot clustering and the erosion effects on cold cathodes is still not possible and needs to be further investigated. The fact that in the Japanese experiments<sup>1,2</sup> the erosion rate is smaller than in ours, can be explained by a smaller average spot current and a larger number of spots.

#### Hot-Arc Cathode

The so-called thermionic attachment occurs when the thoriated (2% ThO<sub>2</sub>) tungsten cathode is heated up and the tip begins to glow very brightly. According to Hügel and Krülle,<sup>4</sup> who experimentally investigated the same type of cathode attachment under similar conditions to those in the MPD thruster, the maximum temperature of the cathode tip amounts to about 3200 K in argon and the average current density varies between about  $2.5 \times 10^6$  and  $1.5 \times 10^7$  A/m<sup>2</sup> for an ambient argon pressure of 20 Torr ( $=2.6 \times 10^{-2}$  bar) and 100 Torr ( $=13.2 \times 10^{-2}$  bar), respectively. Since the maximum temperature does not change very much with the current, one can estimate the sublimation rate by

$$\dot{m}_{\text{subl.}} = A \sqrt{\frac{M}{2\pi RT}} p_v(T) \approx A \times 10^{-4} \quad [\text{kg/s}] \quad (10)$$

where  $p_v(T)$  is the vapor pressure ( $\approx 10^{-1}$  N/m<sup>2</sup>) of tungsten at the surface temperature of  $T=3200$  K;  $A$  is the active, thermionically emitting surface and is given by

**Table 1 Listings of pertinent quantities which yield the same erosion rate of  $0.031 \mu\text{g/C}$**

Erosion rate, $0.031 \mu\text{g/C}$		Flat spot		Hemispherical spot	
$T_s$ [K]	$p_v$ [bar]	$I_s$ [A]	$j_s$ [A/m <sup>2</sup> ]	$I_s$ [A]	$j_s$ [A/m <sup>2</sup> ]
5000	0.04	0.24	$1.1 \cdot 10^{11}$	0.12	$2.0 \cdot 10^{11}$
6000	1.0	0.27	$2.5 \cdot 10^{12}$	0.13	$4.7 \cdot 10^{12}$
7000	10	0.29	$2.3 \cdot 10^{13}$	0.14	$4.4 \cdot 10^{13}$
7500	25	0.30	$5.6 \cdot 10^{13}$	0.14	$1.1 \cdot 10^{14}$
8000	45	0.31	$9.7 \cdot 10^{13}$	0.15	$1.8 \cdot 10^{14}$

$A = I/j$ , i.e., the current measured in  $[A]$  divided by the average current density  $j$  in  $[A/m^2]$ . Therefore, the erosion rate follows by

$$\epsilon = \frac{\dot{m}_{\text{subl.}}}{I} = \sqrt{\frac{M}{2\pi RT}} \frac{p_v(T)}{j} \quad [\text{kg/C}] \quad (11)$$

With an average current density of  $10^7 \text{ A/m}^2$ , which corresponds to the thruster conditions, the erosion rate for the steady-state thruster with a thermionic cathode attachment yields  $10^{-2} \mu\text{g/C}$ . Hence, the calculated rate based on current density and surface temperature measurements is smaller than the directly measured one by about a fraction of one-third. This discrepancy, however, can be easily explained by the error limits of these measurements and by the uncertainties of the vapor pressure curve values. On the other hand, it is hard to understand how such a fairly diffuse thermionic arc-cathode attachment remains stable and does not develop hot spots. Let us discuss this problem very briefly.

The current density on a thermionically emitting cathode surface is governed by the Richardson equation

$$j = A_0 T^2 e^{-\phi/kT} \quad [\text{A/m}^2] \quad (12)$$

where  $A_0$  is the Richardson constant,  $\phi$  the electron work function, and  $k$  the Boltzmann constant. Hence, with increasing surface temperature, the current density increases rapidly. Assuming now that within the diffuse attachment area, due to small fluctuations, the temperature on one spot would increase only slightly above the proper value, the current density would increase in this spot, and along with the current density, due to ohmic heating, the temperature would also increase, and so on. According to Kirchhoff's distribution law, the current would be more and more concentrated until field emission sets in and self-magnetic field effects play a role. In that case, however, the preceding spot theory becomes applicable.

If one assumes now that the bright glowing, seemingly continuous attachment area contains many similar, small hot spots of high current density, one can still explain the measured erosion rate. According to Eq. (9), for such a spotty attachment the overall erosion rate depends only on the individual spot current and the spot temperature. In Table 1 for typical hemispherical and flat spots, several pertinent spot currents,  $I_s$ , and spot temperatures,  $T_s$ , together with the vapor pressure and current density values, are listed, which all yield the same erosion rate of  $0.03 \mu\text{g/C}$ .

As previously mentioned, these extremely high current densities of up to  $10^{12}$  and even  $10^{14} \text{ A/m}^2$  can be explained by field emission, but no longer by pure thermionic emission. The spot current amounts to between 0.1 and about 0.3 A; therefore, the number of spots for a 1000 A arc lies between 3000 and 10,000 spots. Despite this relatively large number, these spots cover only about a fraction of  $10^{-4}$  and even less of the entire growing cathode area.

### Summary

The results of an experimental and theoretical cathode erosion investigation on a pulsed and on a continuously running MPD arc thruster are presented. These results show that on a thoriated tungsten cathode the erosion rates differ considerably. Within the pulsed device, the erosion rate amounts to almost  $17 \mu\text{g/C}$  and remains at about the same amount during the starting phase of the continuously running arc. As soon as the continuous arc becomes steady state, however, which after ignition takes about a fraction of a second or a few seconds until the cathode tip is glowing brightly, the erosion rate drops to  $0.03 \mu\text{g/C}$ .

According to today's knowledge, the attachment on a cold-metal cathode consists of many microspots, the high current density of which can be explained by field emission or thermal field emission. The current-carrying plasma channel, which emanates from such a spot, starts to kink as soon as the spot current increases above a certain level. This kinking or bending now causes the channel to touch the cathode in the vicinity of the spot and eventually leads to a new spot site. This effect causes the spot to split and/or to move discontinuously over the surface. These spots can now cluster together to form more stationary larger ones, which leads to an enhanced erosion. It is shown that the smallest possible overall erosion rate is directly proportional to the spot current and that it is not necessarily a function of the arc current. Therefore, in order to avoid a high erosion rate, the number of spots should be high, while the average spot current should be small. The relatively high cathode erosion rates measured with the pulsed and during the starting phase of the continuous MPD arc thruster are explained by spots that carry a current of about 30–160 A.

The processes occurring on a glowing cathode surface of a steady-state, continuous MPD arc device are discussed and, based on data in the literature, the expected erosion rate determined. Since such a seemingly diffuse thermionic attachment can also be explained by many highly unstable spotty attachments, it is suggested that this so-called thermionically emitting cathode also consists of many tiny hot spots in which field emission is predominant.

### Acknowledgments

This work was partially supported by AFOSR through the European Office of Aerospace Research and Development under Grants 82-0298 and 84-0394, for which the authors are greatly indebted.

### References

- <sup>1</sup>Yoshikawa, T., Kagaya, Y., and Kuriki, K., "Thrust and Efficiency of New K-III MPD Thruster," AIAA Paper 82-1887, 1982.
- <sup>2</sup>Kuriki, K. et al., "MPD Arcjet System Performance Test," IAF Preprint 83-392, 34th IAF Congress, Budapest, Hungary, 1983.
- <sup>3</sup>Clark, K. E. and Jahn, R. G., "Magnetoplasma dynamic Thruster, Erosion Studies, Phase I," Interim Report, AF Contract R 04611-79-C-0039, April 1983.
- <sup>4</sup>Hügel, H. and Krülle, G., "Phänomenologie und Energiebilanz von Lichtbogenkathoden bei Niedrigen Drücken und Hohen Stromstärken," *Beiträge der Plasmaphysik*, Vol. 9, 1969, p. 87.
- <sup>5</sup>Schrade, H. O., Auweter-Kurtz, M., and Kurtz, H. L., "Plasma Thruster Development," Institut für Raumfahrtantriebe, Universität Stuttgart, Rept. IRA 85-P3, April 1985.
- <sup>6</sup>Guile, A. E. and Jüttner, B., "Basic Erosion Processes of Oxidized and Clean Metal Cathodes by Electric Arcs," *IEEE Transactions on Plasma Science*, Vol. PS-8, No. 3, 1980, p. 259.
- <sup>7</sup>Harris, L. P., "Arc Cathode Phenomena," *Vacuum Arcs, Theory and Applications*, edited by J. M. Lafferty, Wiley, New York, 1980.
- <sup>8</sup>Bushik, A. I., Jüttner, B., Pursch, H., and Shilov, A., "Effects of Local Heat Accumulation at the Cathode of Vacuum Arcs," Preprint: Akademie der Wissenschaften der DDR Zentralinstitut für Elektronenphysik, Feb. 1983.
- <sup>9</sup>Djakov, B. E. and Holmes, R., "Cathode Spot Division in Vacuum Arcs with Solid Metal Cathodes," *Journal of Physics D, Applied Physics*, Vol. 4, 1971, p. 504.
- <sup>10</sup>Daalder, J. E., "Diameter and Current Density of Single and Multiple Cathode Discharges in Vacuum," *IEEE Transactions on Power Apparatus and System*, Vol. PAS-93, 1974, p. 1747.
- <sup>11</sup>Roman, W. C., "Some Observations on the Forward and Retrograde Motion of Electric Arcs in Transverse Magnetic Fields," *Proceedings of the VIth International Conference on Phenomena in Ionized Gases*, Paris, 1963, p. 287.
- <sup>12</sup>Murphree, D. L. and Carter, R. P., "Low Pressure Arc Discharge Motion between Concentric Cylindrical Electrodes in a

Transverse Magnetic Field," *AIAA Journal*, Vol. 7, Aug. 1969, pp. 1430-1437.

<sup>13</sup>Good, R. H. and Müller, E. W., "Field Emission," contribution in *Encyclopedia of Physics, Electron-Emission and Gas Discharges I*, edited by S. Flügge, Vol. XXI, Springer-Verlag, Berlin, 1956.

<sup>14</sup>Ecker, G., "Electrode Components of the Arc Discharge," *Ergebnisse der exakten Naturwissenschaften*, Vol. 33, 1961, p. 1.

<sup>15</sup>Kurtz, H. L., Auweter-Kurtz, M., and Schrade, H. O., "Self-Field MPD Thruster Design—Experimental and Theoretical Investigations," AIAA Paper 85-2002, 1985.

<sup>16</sup>Merke, W., "Messungen von Strom- Spannungscharakteristiken Quasi-stationär Betriebener Eigenfeldbeschleuniger," Studienarbeit, Institut für Raumfahrtantriebe, Universität Stuttgart, Stuttgart, 1985.

<sup>17</sup>DiCapua, M. S. and Kurtz, H. L., "Electrolytic Capacitor Power Source Design for Quasi-Steady MPD-Arcs," *Journal of Spacecraft and Rockets*, Vol. 11, Aug. 1974, pp. 554-559.

<sup>18</sup>Schrade, H. O., "Basic Processes of Plasma Propulsion," AFOSR-82-0298, Sept. 1985.

<sup>19</sup>Schrade, H. O., Auweter-Kurtz, M., and Kurtz, H. L., "Analysis of the Cathode Spot of Metal Vapor Arcs," *IEEE Transactions on Plasma Science*, Vol. PS-11, No. 3, 1983, p. 103.

<sup>20</sup>Schrade, H. O., "MPD Effects in Electronic Arcs," AFOSR 82-0298, 1983.

<sup>21</sup>Tuma, D. T. et al, "Erosion Products from the Cathode Spot Region of a Copper Vacuum Arc," *Journal of Applied Physics*, Vol. 49, July 1978, p. 3821.

## *From the AIAA Progress in Astronautics and Aeronautics Series...*

### **SPACECRAFT CONTAMINATION: SOURCES AND PREVENTION – v. 91**

*Edited by J.A. Roux, The University of Mississippi  
and  
T.D. McCay, NASA Marshall Space Flight Center*

This recent Progress Series volume treats a variety of topics dealing with spacecraft contamination and contains state-of-the-art analyses of contamination sources, contamination effects (optical and thermal), contamination measurement methods (simulated environments and orbital data), and contamination-prevention techniques. Chapters also cover causes of spacecraft contamination, and assess the particle contamination of the optical sensors during ground and launch operations of the Shuttle. The book provides both experimental and theoretical analyses (using the CONTAM computer program) of the contamination associated with the bipropellant attitude-control thrusters proposed for the Galileo spacecraft. The results are also given for particle-sampling probes in the near-field region of a solid-propellant rocket motor fired in a high-altitude ground test facility, as well as the results of the chemical composition and size distribution of potential particle contaminants.

*Published in 1984, 333 pp., 6×9, illus., \$39.50 Mem., \$69.50 List; ISBN 0-915928-85-X*

**TO ORDER WRITE: Publications Dept., AIAA, 1633 Broadway, New York, N.Y. 10019**